A colorimetric and ratiometric fluorescent probe with Meldrum's acid as the recognition group for in vitro and in vivo imaging of hypochlorite

Lili Yang, Songsong Ruan, Anqi Zhang, Mengyan Hu, Jie Zhang, Kangjia Sheng, Jing Tian, Yongmin Zhang, Shaoping Wu, Jianli Li

A colorimetric and ratiometric fluorescent probe with Meldrum's acid as the recognition group for *in vitro* and *in vivo* imaging of hypochlorite

Lili Yang[a,b], Songsong Ruan[a,b], Anqi Zhang[a,b], Mengyan Hu[a], Jie Zhang[c], Kangjia Sheng[a,b], Jing Tian[a], Yongmin Zhang[a,b,e], Shaoping Wu[a,b*], Jianli Li[d]

[a] School of Pharmacy; Key Laboratory of Resource Biology and Biotechnology in Western China (Northwest University), Ministry of Education; Biomedicine Key Laboratory of Shaanxi Province, Northwest University, Xi'an 710069, China.

[b] Joint International Laboratory of Glycobiology and Medicinal Chemistry, Northwest University, Xi'an, Shaanxi 710069, China.

[c] Hanbin District First Hospital, Ankang city, Shaan xi province 725000, China.

[d] Key Laboratory of Synthetic and Natural Functional Molecule Chemistry of Ministry of Education, College of Chemistry & Materials Science, Northwest University, Xi'an, Shaanxi 710127, P. R. China.

[e] Sorbonne Université, CNRS, Institut Parisien de Chimie Moléculaire, UMR 8232, 75005 Paris, France.

* Tel.: +86 029 88304569; Fax: +86 029 88304569. E_mail: wushaoping@nwu.edu.cn

Keywords: Fluorescent probe, Ratiometric, Hypochlorite, Meldrum's acid, Fast response, Bioimaging

Abstract:

The detection of ClO^- is vital to comprehend the accurate effect of ClO^- in various diseases and therapeutic interventions by fluorescent probe method. Herein, a special ratiometric probe **DDD** was designed and efficiently synthesized *via* a simple process for hypochlorite detection. The selectivity and sensitivity of probe **DDD** was excellent and the detection was not influenced by other reactive oxygen species. Probe **DDD** exhibited a fast response (< 1 s), wide Stokes Shift (> 100 nm), sensitive limit of detection (78 nM) and two well-separated emission (555 nm and 635 nm). The emission intensities ratio (I_{555}/I_{635}) was linearly enhanced (I_{555}/I_{635} = 0.6273X - 1.9313) with the ClO^- concentration range from 4.0 to 20.0 μM. Furthermore, probe **DDD** has been successfully evaluated in monitoring exogenous HClO in SH-SY5Y neuroblastoma cells and zebrafish larvae with low cytotoxicity, good cell permeability and biocompatibility.

1. Introduction

Reactive Oxygen (ROS) are vital small signaling molecules that intercede many biological events in a serial of physiological processes, such as aging, autoimmunity, cancer, chronic inflammatory diseases and neurodegenerative disorders [1-5]. Hypochlorous acid, an important biologically important weakly acidic ROS which, is partly exists in the form of ClO^- in physiological environment [6]. In living organisms, HOCl is produced mainly by an oxidation reaction between H_2O_2 and Cl^- using the catalysis of myeloperoxidase (MPO) within phagosomes [7,8], and centrally linked to the immune defense systems [9]. However, uncontrolled production of HOCl could lead serious tissue damage and various kinds diseases, for instance hepatic injury [10], atherosclerosis [11], lung injury [12], rheumatoid [13,14], cardiovascular diseases [15], neuron degeneration [16], arthritis [17], and cancer [18,19]. Therefore, the exploitation of reliable and accurate analytical tool for detecting HOCl is vital to illuminate its physiological functions in living systems.

Nowadays, detecting HClO in living systems has attracted extensive interest, especially taking advantage of on the fluorescence confocal imaging techniques because of its high sensitivity, selectivity, rapid response speed and ease of manipulation. Recently, many fluorescent probes have been constructed to detect HOCl in living systems [20]. Although some turn-off fluorescence probes were designed for the exploration and cell imaging of ClO^- based on rhodamine [21,22,23], coumarin [24,25], BODIPY [26] and cyanine [27], such probe applications have some defect due to single wavelength emission and the external environmental influence.

One of the main limitations of single-wavelength emission fluorescent probes is the affect of the signal detection along with probe solution concentration, probe external environment and excitation intensity. However, ratiometric fluorescent probes could effectively assuage these shortcoming [28], it could permit the measurement of fluorescence emission/excitation intensities at two wavelengths, the ratios of emission/excitation intensities would be independent of the external environmental influence [29]. Therefore, it is still great challenge to design and

synthesize novel fluorescent probes that could detect to HOCl in ratiometric type and real time image of the living biosystems.

2,2-Dimethyl-1,3-dioxane-4,6-dione, namely Meldrum's acid, has proven its utility and multifunction in organic chemistry, which is applied in the numerous synthetic methodologies because of very multiple properties and unusual facets of reactivity [30]. To the best of our knowledge, there has been no study on the applications of Meldrum's acid as the fluorescence probe recognition group. On the basis of our previous work [31], a novel colorimetric and ratiometric probe 5-((7-hydroxy-4,5-dihydronaphtho[1,2-b]thiophen-2-yl)methylene)-2,2-dimethyl-1,3-dioxane-4,6-dione(acronym: **DDD**) was reasonable designed and concise synthesized to detect hypochlorite in living cells and zebrafish larvae based on a naphthalenone scaffold and Meldrum's acid as the specially recognition group. Additionally, a proposed recognition mechanism based on addition-ring-opening-elimination reaction was confirmed. Furthermore, probe **DDD** has a fast respond time to hypochlorite over a wide pH range, showing high selectivity over other ROS with excellent stability and good biocompatibility (**Scheme 1**).

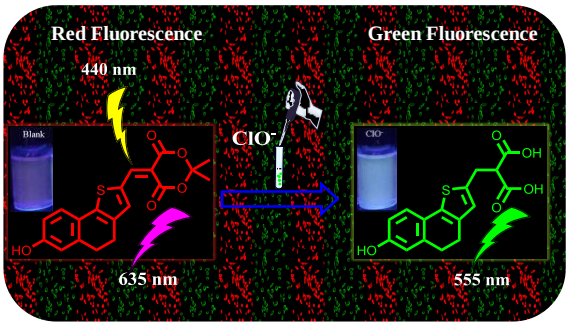

Scheme 1. Strategies to response of probe **DDD**.

2. Materials and methods

2.1. *Materials and instrumentation*

All reagents with analytical grades were obtained from *J&K* Scientific Ltd. (Shanghai China). Hypochlorite stock solution was prepared from the 4 wt% industrial NaClO solution. Stock solutions (1.0 mM) of NO•、$S_2O_3^{2-}$、ClO_4^-、$ONOO^-$、IO_4^-、NO_2^-、NO_3^-、F^-、S^{2-}、CN^-、HSO_3^-、SO_3^{2-}、Mg^{2+}、Ca^{2+}、N_2H_4•H_2O、H_2O_2、Cys、GSH were prepared by proper amounts of salts. The E3 media was made from

NaCl, KCl, $MgSO_4$ and $CaCl_2$. The fluorescence quantum yield of probe **DDD** in different organic solvents was measured at 25 ℃.

The UV-vis spectra were measured on a Shimadzu UV-2550 and the fluorescence spectra were performed using a Hitachi F-7000 spectrophotometer. The cell imaging was collected by the Olympus FV1000 laser confocal fluorescence microscope. The zebrafish imaging was recorded by the Nikon SMZ25 laser confocal fluorescence microscope (Nikon Corporation, Tokyo, Japan).

2.2. *Synthesis of compound 5-((7-hydroxy-4,5-dihydronaphtho[1,2-b]thiophen-2-yl) methylene)-2,2-dimethyl-1,3-dioxane-4,6-dione (**DDD**)*

Compound **1** (50.0 mg, 0.22 mmol, 1.0 equiv.) was dissolved in boiling CH_3CN (5 mL), Meldrum's acid (34.5 mg, 0.24 mmol, 1.1 equiv.) was added with 0.1 mL Et_3N. The mixture was refluxed at 85 ℃ for 2 h, then cooled down to 25 ℃ and stirred for 12 h. The formed precipitate was filtered with neutral filter paper and purified by recrystallization (Yield: 78.8%, R_f = 0.45, PE: EtOAc = 3:1). m.p. > 300 ℃. ^{1}H NMR (600 MHz, DMSO-d_6) δ (ppm): 10.10 (s, 1H), 8.52 (s, 1H), 8.02 (s, 1H), 7.40 (t, *J*=3.8 Hz, 1H), 6.74 (d, *J*=4.1 Hz, 2H), 2.85 (d, *J*=3.6 Hz, 2H), 2.80 (d, *J*=3.9 Hz, 2H), 1.70 (s, 6H). ^{13}C NMR (151 MHz, DMSO-d_6) δ (ppm): 163.05, 160.72, 159.75, 154.17, 147.98, 147.37, 147.98, 147.37, 139.08, 136.81, 131.94, 125.86, 121.19, 104.68, 102.96 , 28.22, 26.83, 26.38, 22.46. FT-IR (KBr) *v*: 3290 (Ar-OH), 2927 (C-H), 1735 (C=O), 1683 (C=O), 1573, 1421(C-H), 1270, 1150, 1023, 823 (Ar C-H) cm^{-1}. HRMS ($C_{19}H_{16}O_5S$): calcd. for $[M-H]^-$ 355.0646; found: $[M-H]^-$ 355.0648. (**Fig. S6-S9**).

2.3. *Titration experiments*

1.0 mM ClO^- standard solution was prepared from 84.5 μL of 4% NaClO solution in 50 mL of ultrapure water for titrations experiments. Probe **DDD** (8.9 mg) was dissolved in 25 mL of absolute ethanol to prepare probe stock solution (1.0 mM). 50 μL of the **DDD** stock solution was diluted to 5 mL (20% EtOH, 10 mM PBS buffer, pH = 7.4) in a glass tube. The other analyte (Cys、GSH、NO•、$S_2O_3^{2-}$、ClO_4^-、$ONOO^-$、IO_4^-、NO_2^-、NO_3^-、F^-、S^{2-}、CN^-、HSO_3^-、SO_3^{2-}、Mg^{2+}、Ca^{2+}、N_2H_4•H_2O、H_2O_2)

was dissolved in water and added to **DDD** stock solution (50 μL) under the same condition. The fluorescence method was used to record the spectra of these solutions.

2.4. *Cytotoxicity experiments*

The cytotoxicity of probe **DDD** was detected by cell counting kit-8 (CCK-8). SH-SY5Y neuroblastoma cells were came from American Type Culture Collection. Cells were added to 96-well plates with a density of 1×10^5 cells per well and cultured in Dulbecco's modified Eagle Medium (DMEM) supplemented with 10% (v/v) fetal bovine serum (FBS) in an incubator (37 ℃, 5% CO_2) for 24 h. The different concentrations of probe **DDD** (0, 5, 10, 15, 20 and 25 μM) were incubated with neuroblastoma cells for 24 h, and then 10 μL CCK-8 was put into each hole of the 96-well plate for 1 h at 37 ℃. Finally, we used a microplate reader to measure the absorbance at 450 nm.

2.5. *Living Cell imaging*

For cell imaging experiments, SH-SY5Y neuroblastoma cells were placed on the laser confocal culture dishes and incubated for 24 h. SH-SY5Y neuroblastoma cells were incubated with probe **DDD** (10 μM) at 36 ℃ for 10.0 min, washed with PBS buffer solution to remove excess **DDD**, and then the different concentrations of ClO^- solution (0, 5, 10, 15, 20, 25 μM, respectively) was added for another 10.0 min. the laser scanning confocal microscope was used to visualize cell.

2.6. *Zebrafish larvae imaging*

Zebrafishes were provided by institute of Hydrobiology (China Zebrafish Resource Center, Chinese Academy of Sciences). To image the exogenous ClO^-, zebrafish larvae (three-days) were put into a 24 well cell culture cluster and incubated in E3 media containing 3 μM probe **DDD** at 28 ℃ for 15 min, the residual probe was washed by E3 media three times, then treated with different concentrations of ClO^- solution (0, 3, 5, 10 μM).

3. Results and discussion

*3.1. Design and synthesis of fluorogenic substrates **DDD***

The synthesis of probe **DDD** was simply achieved in one facile condensation as displayed in **Scheme 2**. Treatment of 6-methoxy-1-tetralone with $POCl_3$ in anhydrous DMF at 90 ℃ gave the intermediate product. The intermediate product reacted with chloroacetaldehyde, Na_2S, K_2CO_3 in anhydrous DMF to give the aldehyde **1'** [32,33]. Compound **1** (see **Scheme S1**) was obtained by demethylation of aldehyde **1'** with BBr_3 [34], then reacted with Meldrum's acid using Et_3N as catalyst in anhydrous CH_3CN to obtain probe **DDD** [35].

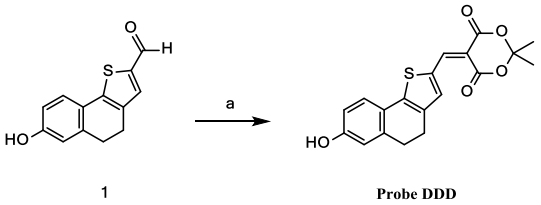

1 **Probe DDD**

Scheme 2. Reagent and conditions: a. Meldrum's acid, Et_3N, CH_3CN, 78.8%.

3.2 Photophysical properties study

The emission characteristics of probe **DDD** were studied in EtOH-PBS solution (pH 7.4). Then the spectroscopic propertie of **DDD** was evaluated in various polarity solvents including EtOH, MeOH, DMF, DMSO. On the other hand, the fluorescence quantum yield of **DDD**-ClO^- adduct in different organic solvents was measured at 25 ℃ using the 0.1 M fluorescein (Φ_f = 0.79) as a standard. The calculated fluorescence quantum yield for **DDD**-ClO^- adduct in different organic solvents was depicted in **Table 1**.

Table 1. Optical properties of **DDD**-ClO^- in different organic solvents.

Solvent	λ_{abs}	ε_{max}	λ_{em}	$\Phi_{F(X)}$	Stokes shift	
	nm	$M^{-1}•cm^{-1}$	nm		nm	cm^{-1}
DMF	487	25600	565	0.41	125	5028
DMK	477	32000	563	0.56	123	4965
MeOH	499	35200	561	0.57	121	4902
THF	483	45700	561	0.78	121	5902
EtOH	499	30500	556	0.75	116	4741
EtOAc	478	67700	544	0.12	104	4345
DCM	482	60800	544	0.21	104	4345
H_2O	424	27400	542	0.37	102	4277
TCM	483	74900	540	0.23	100	4208
ACN	473	21500	530	0.70	90	3859
DMSO	492	20100	520	0.48	80	3496

UV-vis and emission spectra of probe **DDD** in the absence and presence of hypochlorite are shown in **Fig.1**. Probe **DDD** (10 μM) alone showed an absorption band with a peak at 495 nm in EtOH-PBS solution (pH 7.4) at 25 ^{o}C with the unadjusted inner filter effect [36]. With the addition of hypochlorite (20 μM), a red shift of 80 nm was observed, a new band centered at 575 nm (**Fig. 1a**). As shown in **Fig. 1b**, the free probe **DDD** exhibited two emission peaks at 555 nm and 635 nm when excited at 440 nm. Stimulation of probe **DDD** (10 μM) with hypochlorite (20 μM) generated a strong fluorescence peak at 555 nm and accompanied by the peak decrease at 635 nm.

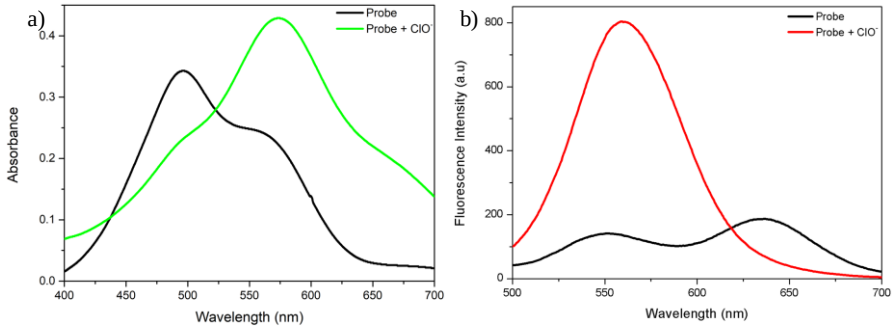

Fig. 1 UV-vis absorption (a) and emission spectra (b) of probe **DDD**（10 μM） in the absence and presence of ClO^- (20 μM) with 20% EtOH solution (10 mM PBS buffer, pH 7.4). λ_{ex}= 440 nm, slits: 5.0 nm/5.0 nm, volt: 700 v.

*3.3. UV-vis and fluorescence spectrum of probe **DDD** react with hypochlorite*

The UV-vis spectra of probe **DDD** (10 μM) upon titration with hypochlorite were measured in EtOH-PBS solution (pH 7.4) (**Fig. 2**) for further insight into the interaction between probe **DDD** and hypochlorite. When hypochlorite was continuously added in probe **DDD** solution, the absorbance value at 495 nm decreased sharply and the peak at 575 nm increased significantly, which induced a colour change of the test solution from rose red to purple under simulated daylight irradiation (**Fig. 3a**). UV-visible titration experiments between the ratios of absorbance value at 575 nm and 495 nm ($A_{575\ nm}/A_{495\ nm}$) and the concentration of hypochlorite anions showed high coefficient (R^2 = 0.9915) in 0 ~ 12 μM with good linearity. These data revealed that probe **DDD** could be used for colorimetric detection hypochlorite under visible light.

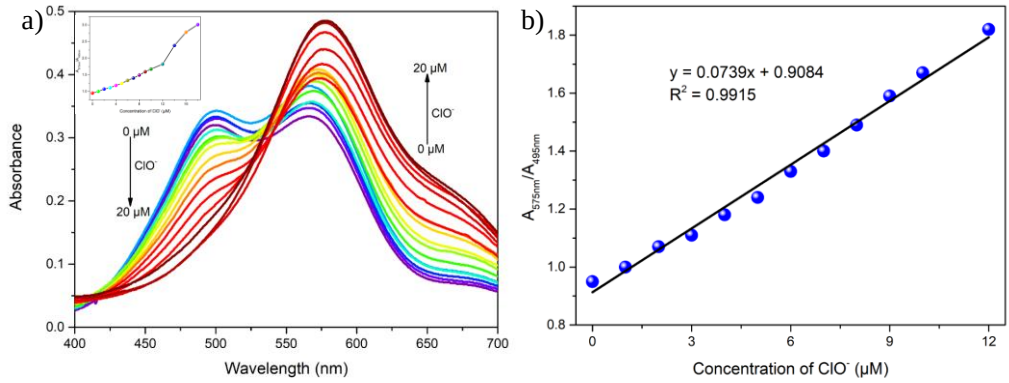

Fig. 2 a) UV-vis spectra of probe **DDD** (10 μM) in the presence of various concentrations of ClO^- (0-12 μM) with 20% EtOH solution (10 mM PBS buffer, pH 7.4). Each spectrum was recorded after 1 min at 25 ℃; b). Plot of absorbance ratios of probe **DDD** as a function of ClO^- concentration at 575 nm and 495 nm (A_{575nm}/A_{495nm}).

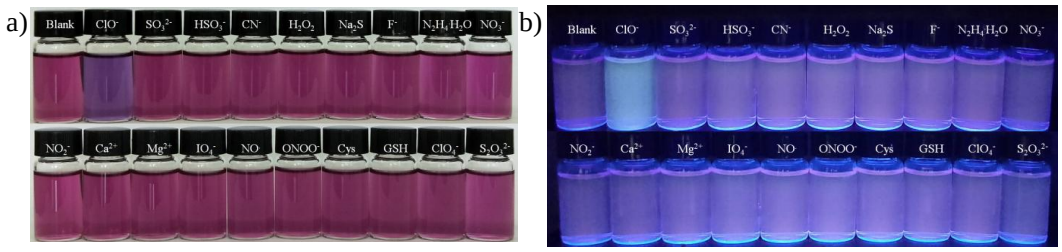

Fig. 3 Image of color change of probe **DDD** (10 μM) after the addition of different ions (10 μM) in 20% EtOH solution (10 mM PBS buffer, pH 7.4) at 25 ℃. (a) Color of **DDD** in the absence/presence of ClO^- under daylight lamp. (b) Fluorescence images of **DDD** in the absence/presence of ClO^- under fluorescent lamp.

Next, the fluorescence changes of hypochlorite titration with probe **DDD** were investigated in EtOH-PBS solution (pH 7.4). **Fig. 4** illustrated variations of fluorescence spectra of probe **DDD** upon addition of different concentrations hypochlorite. As we can seen from **Fig. 4a**, the emission maximum of probe **DDD** underwent a blue-shift from 635 to 555 nm upon an increasing amount of hypochlorite. The intensity ratios of fluorescence at 555 nm and 635 nm ($I_{555\ nm}/I_{635\ nm}$) as a function of the concentration of hypochlorite increased linearly in the scope of 4 ~ 20 μM hypochlorite anions (R^2 = 0.9911) (**Fig. 4b**). Additionally, a color of the test solution change from lavender to blue was observed under fluorescent lamp. The minimum detection limit of a signal-to-noise ratio was then calculated to be 78 nM from eleven blank solutions (**Table S2**). These outcomes illustrated that probe **DDD** have excellent potential for qualitative and quantitative analysis of hypochlorite level

along with luxuriously sensitivity. Compared with UV-vis method, the fluorescence method of the detection hypochlorite has a wider linear range and lower detection limit.

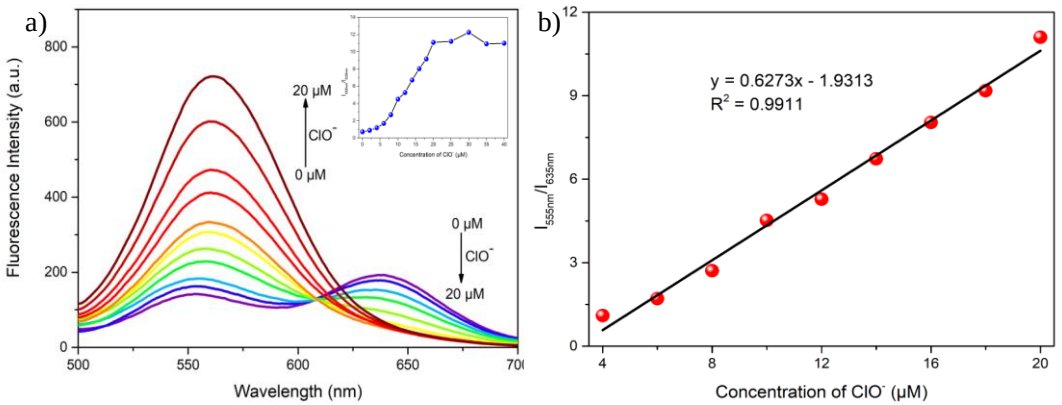

Fig. 4 a) Fluorescence spectra of probe **DDD** (10 μM) in the presence of various concentrations of ClO^- (0-20 μM) in 20% EtOH solution (10 mM PBS buffer, pH 7.4) at 25 ℃; b). Plot of emission ratios at 555 nm and 635 nm ($I_{555\ nm}/I_{635\ nm}$) of probe **DDD** as a function of ClO^- concentration. λ_{ex}= 440 nm, slits: 5.0 nm/5.0 nm, volt: 700 v.

3.4. Selectivity experiment

The selectivity of probe **DDD** toward ClO^- was evaluated by investigating a variety of biological relevant species, including ROS, RSS, cations and anions. As diagrammed in **Fig. 5a**, when ClO^- was added, the fluorescence intensity of probe **DDD** at 555 nm significantly increased. On the other hand, the fluorescence intensity exhibited no obvious change upon addition of other analytes at considerable concentrations.

As shown in **Fig. 5b**, the anti-interference ability of **DDD** was examined to other analytes. The detection of ClO^- did not interfere under all the competing analytes, these analytical results indicated that probe **DDD** has excellent selectivity for ClO^- over a various interfering species that can be exist in complex biological systems.

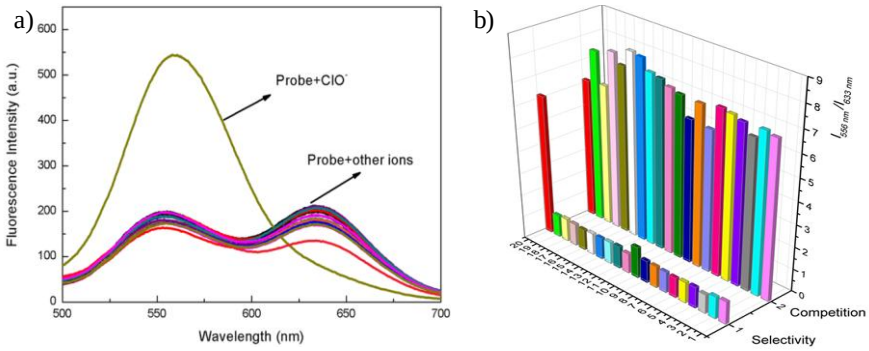

Fig. 5 a) Fluorescence spectra of probe **DDD** (10 μM) upon addition of 20 μM ClO^- and 19 kinds of 10 μM other ions (Cys、GSH、NO•、$S_2O_3^{2-}$、ClO_4^-、$ONOO^-$、IO_4^-、NO_2^-、NO_3^-、F^-、S^{2-}、CN^-、HSO_3^-、SO_3^{2-}、Mg^{2+}、Ca^{2+}、N_2H_4•H_2O、H_2O_2) in 20% EtOH solution (10 mM PBS buffer, pH 7.4). λ_{ex}= 440 nm, slits: 5.0 nm/5.0 nm, volt: 700 v; b) Pillars in the front row represent fluorescence response of the probe **DDD** to the ions of interest. The pillars in the back row represent the subsequent addition 20 μM ClO^- to the solution containing probe **DDD** and other ions, respectively.

3.5. Time influences and pH-dependent

We also investigated the fluorescence intensity alterations of probe **DDD** toward hypochlorite with a time-dependent by kinetic study. As showed in **Fig. 6a**, the intensity ratios of fluorescence at 555 nm and 635 nm (I_{555nm}/I_{635nm}) increased significantly and reached a plateau within one second. Additionally, the fluorescence intensity of **DDD**-ClO^- adduct almost remained constant within 30 min, indicating that probe **DDD** was a "fast response" fluorescent probe for real time monitoring hypochlorite levels *in vivo* and *in vitro*.

On the other hand, The pH tolerance of the free probe **DDD** and **DDD**-ClO^- adduct was researched by adding PBS buffers, which were prepared in the pH range from 3.0 to 14.0 in 20% EtOH mixed solution (**Fig. 6b**). The notable changes fluorescence intensity of the free probe **DDD** could not cause in the pH range from 3.0 to 10.0. At the same time, Probe **DDD** itself was very stable in the pH range of 3.0 to 10.0. When hypochlorite was added in the **DDD** solution, fluorescence intensity increased significantly in the pH range from 7.0 to 13.0. These results demonstrated that probe **DDD** could tolerate a wide range of pH change and could be used in biological systems.

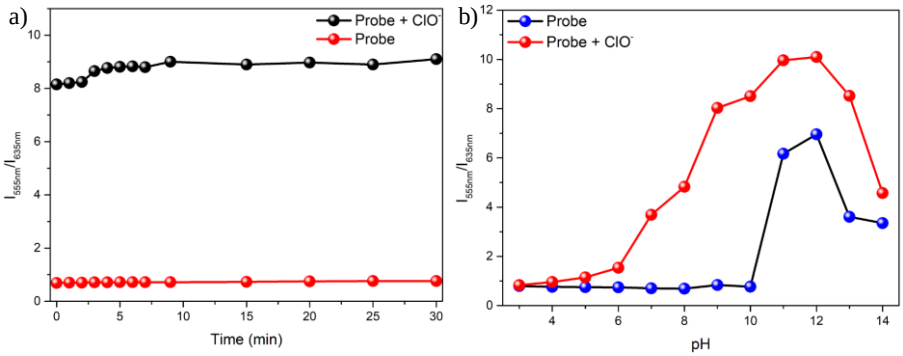

Fig. 6 a) Reaction time profile between probe **DDD** (10 μM) and ClO^- (20 μM) in 20% EtOH solution (10 mM PBS buffer, pH 7.4). λ_{ex}= 440 nm, slits: 5.0 nm/5.0 nm, volt: 700 v; b) Fluorescence intensity ratio of probe **DDD** (10 μM) without or with of ClO^- (20 μM) at different pH. in 20% EtOH solution (10 mM PBS buffer, pH 7.4). λ_{ex}= 440 nm, slits: 5.0 nm/5.0 nm, volt: 700 v.

3.6 Recognition mechanism study

The reaction of **DDD** with hypochlorite of the mechanism was shown in **Scheme 3**. ClO^- as a hard nucleophile attack to carbon-carbon double bond and the addition product **3** is observed. Next water reacted as nucleophilic reagent on the carbonyl to give intermediate **4** which, after proton transfer and hydrolysis, gave malonic acid derivative **5**. To support our speculation, the reaction of **DDD** (50 μM) and ClO^- (100 μM) was carried out in MeOH solution at 0 ^oC for 3 min, after that the reaction mixture was diluted appropriately and checked to high resolution mass spectroscopy, where two anticipated molecular ion peaks at m/z 317.0760 and 355.0630, representing malonic acid derivative **5** ($C_{16}H_{14}O_5S$, Exact Mass: $[M-H]^-$ 317.0484) and **DDD** ($C_{19}H_{16}O_5S$, $[M-H]^-$ 355.0640) were obtained, respectively (**Fig. S10**).

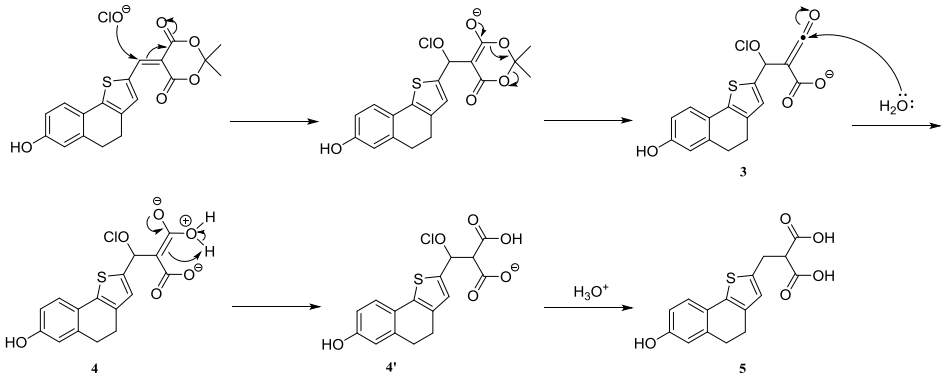

Scheme 3. Proposed mechanism for the reaction of probe **DDD** with ClO^-.

3.7. Cytotoxicity of living cells and fluorescence imaging

CCK-8 method was used to evaluate the cytotoxicity of probe **DDD**. As displayed in **Fig. S11**, the cell viability was up to 95% when 10 μM probes were incubated with the SH-SY5Y neuroblastoma cells for 24 h. These cytotoxicity results showed that probe **DDD** possess low cytotoxicity and excellent biocompatibility at range of 0 ~ 25 μM in living cells.

On the basis of these above experiments, the imaging exogenous ClO^- of probe **DDD** in living cells was explored (**Fig. 7**). After the SH-SY5Y neuroblastoma cells were mixed with probe **DDD** (10 μM) for 10 min, the bright red fluorescence and weak green fluorescence was observed in living cells. Then, an apparent increase was checked in green channel fluorescence when cells treated with various concentration of ClO^- (10 μM, 20 μM and 30 μM) for 10 min, but the red channel fluorescence was made a dramatic decline. The phenomenon displayed that probe **DDD** can detect hypochlorite in living cells, possessing great cell-membrane permeableness and good ratio imaging *in vivo*.

We also used Image J software to calculate the fluorescence signal ratio of SH-SY5Y neuroblastoma cells in two channels (F_{green}/F_{red}), and the consequences appearance that the fluorescence intensity ratio of cells increased with the increase of ClO^- concentration (**Fig. 7b**). Therefore, these data indicated that probe **DDD** not only has good membrane permeability in biological applications, but also provides a ratio response to changes in ClO^- levels in living cells.

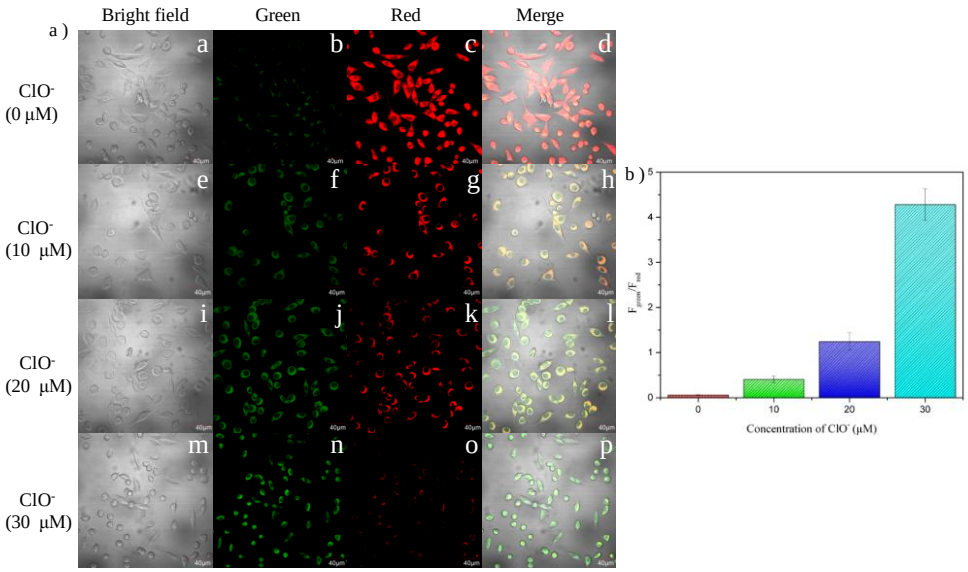

Fig. 7 a) Imaging of exogenous ClO^- in SH-SY5Y neuroblastoma cells. SH-SY5Y neuroblastoma cells was fed with probe **DDD** (10 μM) for 10 min (a-d); the cells were pretreated with probe in DMEM for 10 min and was then incubated with 10 μM ClO^- (e-h), 20 μM ClO^- (i-l) and 30 μM ClO^- (m-p) for 10 min; b) Fluorescence intensity ratios in two channels (F_{green}/F_{red}) in Fig 7a, $*p < 0.05$. The results are presented as means ±SE with replicates $n = 5$. The calculations were conducted by Image J software. Red channel (λ_{ex}= 488 nm, λ_{em}=570-670 nm), Green channel (λ_{ex}= 405 nm, λ_{em}= 470-570 nm).

3.8 Imaging of exogenous ClO^- in vitro

Mostly, the zebrafish larvae experimental results were also suitable for human body [37] because of 87% homologous genes with human [38]. To evaluate the potential application of probe **DDD** for imaging exogenous ClO^- *in vivo*, we used zebrafish larvae as the animal mode in this work. As could be seen from **Fig. 8**, the zebrafish larvae showed no fluorescence without probe **DDD** and ClO^-. After the zebrafish larvae was incubated with probe **DDD** (3 μM) for 15 min, next the residual probe was rinsed by E3 media three times, the zebrafish larvae displayed bright red fluorescence and weak green fluorescence. Then zebrafish larvae caused an evident fluorescence increase in the green channel treated with 3, 5 and 10 μM ClO^- for 15 min, along with a distinct fluorescence weakening in red channel. The imaging results indicated that probe **DDD** could exhibit the ratio fluorescence response of hypochlorite in living bodies and provided the new avenue of whole-organism investigations.

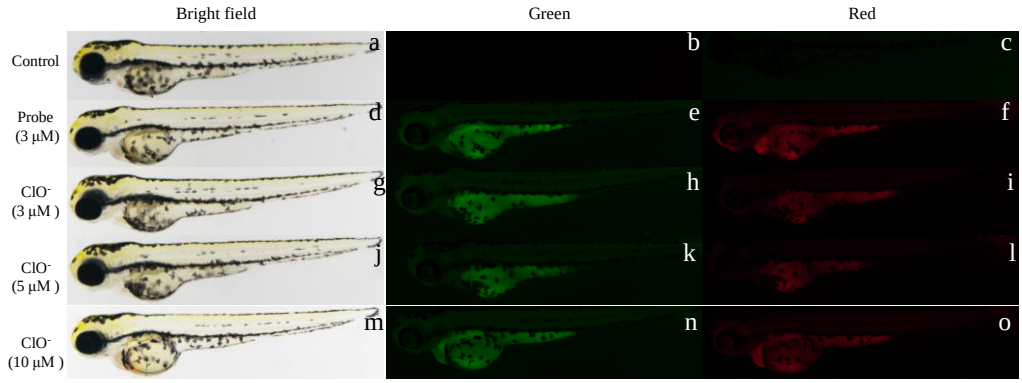

Fig. 8 Fluorescence images of exogenous ClO^- in zebrafish larvae incubated with probe **DDD** for 15 min. The control was without probe **DDD** and ClO^- (a-c); the zebrafish larvae was fed with the probe **DDD** (3 μM) for 15 min (d-f); the zebrafish larva was pretreated with probe in E3 media for 15 min and was then incubated with 3 μM ClO^- (g-i), 5 μM ClO^- (j-l) and 10 μM ClO^- (m-o) for 15 min. red channel (λ_{ex}= 488 nm, λ_{em}= 570-670 nm), green channel (λ_{ex}= 405 nm, λ_{em}= 470-570 nm).

4. Conclusion

In summary, probe **DDD** with Meldrum's acid reporting moiety was designed and synthesized to detect ClO^-. Probe **DDD** demonstrated excellent sensitivity and selectivity toward hypochlorite and exhibited a fast response, a large Stokes Shift, sensitive limit of detection, physiologically pH range and two well-separated emission (555 nm and 635 nm) which was prepared *via* a simple process. Additionally, the probe had low cytotoxicity, good cell permeability and biocompatibility, and has been used in fluorescence confocal imaging in living cells and zebrafish larvae. Moreover, we anticipate that the novel fluorescence probe **DDD** could be used to advance reveal basic physiology information about ClO^- in living organization.

Acknowledgements

We sincerely thank the National Natural Science Foundation of China (No. 21572177), Scientific Research Program Funded by Shaanxi Provincial Education Department (No. 18JK0774), the International Science & Technology Cooperation Program of Shaanxi Province (No. 2019KWZ-001), Biomedicine Key Laboratory of Shaanxi Province (No. 2018SZS41), and Training Program of Innovation for Undergraduates of Northwest University (No. 2019230).

Appendix A. Supplementary data

Supplementary data associated with this article can be found, in the online version, at http://

References

[1] Diehn M, Cho RW, Lobo NA, Kalisky T, Dorie MJ, Kulp AN, Qian D, Lam JS, Ailles LE, Wong M, Joshua B, Kaplan MJ, Wapnir I, Dirbas FM, Somlo G, Garberoglio C, Paz B, Shen J, Lau SK, Quake SR, Brown JM, Weissman IL, Clarke MF. Association of reactive oxygen species levels and radioresistance in cancer stem cells. Nature 2009; 458: 780-3.

[2] Drög W. Free radicals in the physiological control of cell function. Physiol Rev 2002; 82: 47-95.

[3] Uttara B, Singh AV, Zamboni P, Mahajan RT. Oxidative stress and neurodegenerative diseases: a review of upstream and downstream antioxidant therapeutic options. Curr Neuropharmacol 2009; 7: 65-74.

[4] Hensley K, Robinson KA, Gabbita SP, Salsman S, Floyd RA. Reactive oxygen species, cell signaling, and cell injury. Free Radical Biol Med 2000; 28: 1456-62.

[5] Valko M, Leibfritz D, Moncol J, Cronin MT, Mazur M, Telser J. Free radicals and antioxidants in normal physiological functions and human disease. Int J Biochem Cell Biol 2007; 39: 44-84.

[6] Shepherd J, Hilderbrand SA, Waternan P, Heinecke JW, Weissleder R, Libby P. A fluorescent probe for the detection of myeloperoxidase activity in atherosclerosisassociated macrophages. Chem Biol 2007; 14: 1221-31.

[7] Fang FC. Antimicrobial reactive oxygen and nitrogen species: concepts and controversies. Nat Rev Microbiol 2004; 2: 820-32.

[8] Roos D, Winterbourn CC, Immunology. Lethal weapons. Science 2002; 296: 669-71.

[9] Henderson JP, Byun, Heinecke JJW, Molecular chlorine generated by the myeloperoxidase-hydrogen peroxide-chloride system of phagocytes produces 5-chlorocytosine in bacterial RNA. J Biol Chem 1999; 274: 33440-8.

[10] Hasegawa T, Malle E, Farhood A, Jaeschke H. Generation of hypochlorite-modified proteins by neutrophils during ischemia-reperfusion injury in rat liver: attenuation by ischemic preconditioning . Am J Physiol Gastrointest Liver Physiol 2005; 289: 760-7.

[11] Daugherty A, Dunn J, Rateri D, Heinecke JW. Myeloperoxidase, a catalyst for lipoprotein oxidation, is expressed in human atherosclerotic lesions. J Clin Invest 1994; 94: 437-44.

[12] Hammerschmidt S, Buchler N, Wahn H. Tissue lipid peroxidation and reduced glutathione depletion in hypochlorite-induced lung injury. Chest 2002; 121: 573-81.

[13] Wu SM, Pizzo SV. α2-Macroglobulin from rheumatoid arthritis synovial fluid: functional analysis defines a role for oxidation in inflammation. Arch Biochem Biophys 2001; 391: 119-26.

[14] Koide Y, Urano Y, Hanaoka K, Terai T, Nagano T. Development of an Si-rhodamine- based far-red to near-infrared fluorescence probe selective for hypochlorous acid and its applications for biological imaging. J Am Chem Soc 2011; 133: 5680-2.

[15] Sugiyama S, Kugiyama K, Aikawa M, Nakamura S, Ogawa H, Libby P. Hypochlorous acid, a macrophage product, induces endothelial apoptosis and tissue factor expression: involvement of myeloperoxidase-mediated oxidant in plaque erosion and thrombogenesis. Arterioscler Thromb Vasc Biol 2004; 24: 1309-14.

[16] Yap YW, Whiteman M, Cheung NS. Chlorinative stress: an underappreciated mediator of neurodegeneration? Cell Signal 2007; 19: 219-28.

[17] Steinbeck MJ, Nesti LJ, Sharkey PF, Parvizi J. Myeloperoxidase and chlorinated peptides in osteoarthritis: potential biomarkers of the disease. J Ortho Res 2007; 25: 1128-35.

[18] Podrez EA, Abu-Soud HM, Hazen SL. Myeloperoxidase-generated oxidants and atherosclerosis. Free Radic Biol Med 2000; 28: 1717-25.

[19] Pattison DI, Davies MJ. Evidence for rapid inter- and intramolecular chlorine transfer reactions of histamine and carnosine chloramines: implications for the prevention of hypochlorous-acid-mediated damage. Biochemistry 2006; 45: 8152-62.

[20] (a) Li X, Gao X, Shi W, Ma H. Design strategies for water-soluble small molecular chromogenic and fluorogenic probes. Chem Rev 2014; 114: 590-659; (b) Ashton TD, Jolliffe KA, Pfeffer FM. Luminescent probes for the bioimaging of small anionic species in vitro and in vivo. Chem Soc Rev 2015; 44: 4547-95; (c) Tang Y, Lee D, Wang J, Li G, Yu J, Lin W, Yoon J. Development of fluorescent probes based on protection-deprotection of the key functional groups for biological imaging. Chem Soc Rev 2015; 44: 5003-15; (d) Yuan L, Lin W, Song J, Yang Y. Development of an ICT-based ratiometric fluorescent hypochlorite probe suitable for living cell imaging. Chem Commun 2011; 47: 12691-3; (e) Zhang YR, Liu Y, Feng X, Zhao BX. Recent progress in the development of fluorescent probes for the detection of hypochlorous acid. Sensor. Actuat B: Chem 2017; 240: 18-36; (f) zhang HF, Huo FJ, Zhang YB, Yin CX. Mono- or di- naphthalimides as fluorophore to detect hypochlorousacid (HOCl) by ratiometric fluorescent signal and their biologicalapplication. Sens Actuators B 2018; 269; 180-8; (g) Xiong KM, Huo FJ, Yin CX, Chu YY, Yang YT, Chao JB, Zheng AM. A novel recognition mechanism supported by experiment and theoretical calculation for hypochlorites recognition and its practical application[J]. Sens Actuators B: Chem 2016; 224; 307-14; (h) Yue Y, Huo F, Cheng F, Zhu X, Mafireyi T, Strongin RM, Yin CX. Functional synthetic probes for selective targeting and multi-analyte detection and imaging. Chem Soc Rev 2019; 48; 4155-77; (i) Li JW, Yin CX , Liu T , Wen Y, Huo FJ. A new mechanism-based fluorescent probe for the detection of ClO^- by UV–vis and fluorescent spectra and its applications. Sens Actuators B 2017; 252; 1112-7; (j) Chen YH, Wei TW, Zhang ZJ, Zhang W, Lv J, Chen TT, Chi B, Wang F, Chen XQ. A mitochondria-targeted fluorescent probe for ratiometric detection of hypochlorite in living cells. Chin. Chem. Lett., 2017; 28: 1957-1960.

[21] Zhou J, Li LH, Shi W, Gao XH, Li XH, Ma HM. HOCl can appear in the mitochondria of macrophages during bacterial infection as revealed by a sensitive mitochondrial-targeting

fluorescent probe. Chem Sci 2015; 6: 4884-8.

[22] Zhang YR., Liu Y, Fang X, Zhao BX. Recent progress in the development of fluorescent probes for the detection of hypochlorous acid. Sens. Actuators B: Chem 2017; 240: 18-36.

[23] (a) Hou JT, Wu MY, Li K, Yang J, Yu KK, Xie YM, Yu XQ. Mitochondria-targeted colorimetric and fluorescent probes for hypochlorite and their applications for in vivo imaging. Chem Commun 2014; 50: 8640-3; (b) Xia Y, Liu XY, Wang D, Wang ZC, Liu Q, Yu HB, Zhang MY, Song YT. A fluorometric and mitochondrion-targetable probe for rapid, naked-eye test of hypochlorite in real samples. Chin. Chem. Lett., 2018; 29: 1517-1520.

[24] Li XH, Gao XH, Shi W, Ma HM. Design strategies for water-soluble small molecular chromogenic and fluorogenic probes. Chem Rev 2014; 114: 590-659.

[25] Li GP, Zhu DJ, Liu Q, Xue L, Jiang H. A strategy for highly selective detection and imaging of hypochlorite using selenoxide elimination. Org Lett 2013; 15: 2002-5.

[26] Kolemen S, Engin UA. Reaction-based BODIPY probes for selective bio-imaging. Coord. Chem Rev 2017; 354: 121-34.

[27] Lin QS, Huang YL, Fan XX, Zheng XL, Chen XL, Zhan XQ, Zheng H. A ratiometric fluorescent probe for hypochlorous acid determination: excitation and the dual-emission wavelengths at NIR region. Talanta 2017; 170: 496-501.

[28] Yuan L, Lin WY, Zheng KB, Zhu S. FRET-based small-molecule fluorescent probes: rational design and bioimaging applications. Acc Chem Res 2013; 46: 1462-73.

[29] Kikuchi K, Takakusa H, Nagano T. Recent advances in the design of small moleculebased FRET probes for cell biology. Trend Anal Chem 2004; 23: 407-15.

[30] Pair E, Cadart T, Levacher V, Brière JF. Meldrum's acid: a useful platform in asymmetric organocatalysis. Chemcatchem 2016; 8: 1882-90.

[31] (a) Ning YY, Cui JH, Wang XQ, Xiao CN, Wu SP, Li JL, Zhang YM. De novo design and synthesis of a novel colorimetric fluorescent probe based on naphthalenone scaffold for selective detection of hypochlorite and its application in living cells. Sens Actuators B 2018; 269: 322-30; (b) Ning YY, Wang XQ, Yang LL, Xiao CN, Wu SP, Li JL, Zhang YM. A novel colorimetric and fluorescence turn-on pH sensor with a notably large Stokes Shift for its application. New J Chem 2018; 42: 14510-6.

[32] Chen H, Tang YH, Ren MG, Lin WY. Single near-infrared fluorescent probe with high- and low-sensitivity sites for sensing different concentration ranges of biological thiols with distinct modes of fluorescence signals. Chem Sci 2016; 7: 1896-903.

[33] Herbivo C, Comel A, Kirsch G, Manuela M, Raposo M. Synthesis of 5-aryl-5'-formyl-2, 2'-bithiophenes as new precursors for nonlinear optical (NLO) materials. Tetrahedron 2009; 65: 2079-86.

[34] Tedesco R, Youngman MK, Wilson SR, Katzenellenbogen JA. Synthesis and evaluationof hexahydrochrysene and tetrahydrobenzofluorene ligands for the estrogen receptor. Bioorg Med Chem Lett 2001; 11: 1281-4.

[35] Farat OK, Farat SA, Ananyev IV, Okovytyy SI. Novel xanthene push-pull chromophores and

luminophores: Synthesis and study of their spectral properties. Tetrahedron 2017; 73: 7159-68.

[36] (a) Lewandowska-Andralojc A, Marciniak B. Five Major Sins in Fluorescence Spectroscopy of Light-Harvesting Hybrid Materials. ACS Energy Lett 2019; 4: 1898-901. (b) Deshmukh A, Bandyopadhyay S, James A, Patra A. Trace level detection of nitroanilines using a solution processable fluorescent porous organic polymer. J Mater Chem C 2016 ; 4: 4427-33.

[37] Drabsch Y, He S, Zhang L, et al. Transforming growth factor-β signalling controls human breast cancer metastasis in a zebrafish xenograft model. Breast Cancer Res 2013; 15: 106-19.

[38] Liu YB, Li DL, Yuan Z. Photoacoustic tomography imaging of the adult zebrafish by using unfocused and focused high-frequency ultrasound transducers. Appl Sci 2016; 6: 392-9.